Open Archive Toulouse Archive Ouverte

OATAO is an open access repository that collects the work of Toulouse researchers and makes it freely available over the web where possible

This is an author's version published in: http://oatao.univ-toulouse.fr/20661

Official URL:

https://doi.org/10.1108/09615530810879710

Any correspondence concerning this service should be sent to the repository administrator: tech-oatao@listes-diff.inp-toulouse.fr

Numerical study of thermosolutal convection with Soret effect in a square cavity

L. Kaffel Rebaï

Unité de Recherche en Mécanique et Energétique,
Ecole Nationale d'Ingénieurs de Tunis, Tunis, Tunisie

A. Mojtabi

IMFT, Université Paul Sabatier, Toulouse, France

M.J. Safi

Unité de Recherche en Mécanique et Energétique,
Ecole Nationale d'Ingénieurs de Tunis, Tunis, Tunisie, and

A.A. Mohamad

Department of Mechanical and Manufacturing Engineering,
University of Calgary, Canada

Abstract

Purpose – The purpose of this paper is to present a numerical and an analytical study of the thermohaline convection with Soret effect in a square enclosure filled with a binary fluid mixture.

Design/methodology/approach – The horizontal boundaries of the enclosure are impermeable and heated from below while its vertical walls are assumed to be adiabatic and impermeable. The Navier-Stokes equations under the Boussinesq-Oberbeck approximation are solved numerically. The results are given for different values of the separation ratio. The critical Rayleigh number at the onset of convection is determined analytically and numerically. The Hopf frequency at the onset of convection is obtained.

Findings – The existence of two stable stationary bifurcation branches is illustrated. Furthermore, it is shown that the existence of stable traveling waves in the transition from one branch to the other depends on the value of the separation ratio. For some values of Rayleigh number, asymmetric flows are observed. A good agreement is found between the numerical solution and analytical analysis.

Originality/value – The present work is the first to consider thermosolutal convection with Soret effect in a square enclosure.

Keywords Convection, Thermal stability, Numerical analysis

Paper type Research paper

Nomenclature

A	= aspect ratio	D	= mass diffusion coefficient
a_{ij}, b_{ij}, c_{ij}	= spectral coefficients	f^{osc}	= oscillation frequency
C	= concentration	g	= acceleration of gravity
c	= perturbed concentration	H	= height of cavity
D_{T}	= thermal diffusion coefficient	N, M	= truncate numbers

P_m	= pressure	ψ	= perturbed stream function
$\mathbf{V}$	= velocity vector (u, w)	κ	= thermal diffusivity
T	= temperature	ν	= viscosity
		ρ	= density
Dimensionless numbers		θ	= perturbation of temperature
Ra	= thermal Rayleigh number	τ	= period
Le	= Lewis number	ω	= Hopf frequency
Pr	= Prandtl number		
Ψ_S	= separation ratio	*Subscripts and superscripts*	
		Crit	= critical value
Greek symbols		e	= equilibrium
β_T	= coefficient of thermal expansion	0	= initial state
β_S	= coefficient of concentration expansion	1	= value in the bottom
		2	= value in the top
Ψ	= stream function	max	= maximal value

1. Introduction

Rayleigh-Benard convection in binary mixtures has recently attracted much attention due to it is importance in many industrial applications such as space, petroleum and biomedical technologies. The coupling between concentration and temperature fields leads to more complex flow structures and need some further developments. Few investigations on the topics were reported in the 1960s and 1970. However, theoretical studies (Veronis, 1965, 1968; Nield, 1967; Hurle and Jakeman, 1971; Schechter *et al.*, 1972) and experimental one (Lhost and Platten, 1988, 1989a, b) allowed the calculation of critical Rayleigh numbers, wave numbers and frequencies as a function of the Soret coefficient $S = D_T/D$ or some equivalent parameter, such as the separation ratio:

$$\Psi_S = \frac{D_T}{D} C_0(1 - C_0) \frac{\beta_S}{\beta_T}$$

These studies showed a great variety of convective flows; especially they reported the existence of unstable traveling waves (TW) (Hopf bifurcation) at the onset of convection. Rehberg and Ahlers (1985) proved that the heat-transport measurements in a mixture contained in a porous medium and heated from below show a bifurcation to steady or oscillatory flow, depending on the mean temperature. Knobloch (1986) studied the problem of two dimensional oscillatory convection for a binary fluid mixture in an infinite plane porous layer heated from below. He found different type of convective flows, standing waves and modulated TW. Stable TW are preferred mod near the onset of convection. Other authors (Lhost and Platten, 1988, 1989a, b) found a stable state characterized by a system of stable TW just after the critical point. They determined the bifurcation point of the stationary stable state (SOC) as the Rayleigh number increases. Modulated TW were also observed experimentally (Heinrichs *et al.*, 1987).

Most of the thermosolutal studies related to the linear stability analysis have considered an infinite horizontal fluid layer heated from below. Veronis (1965) studied the possibility of finite amplitude convection. It was demonstrated that a sub-critical instability might set in at a Rayleigh number smaller than the values predicted by the principle of stability exchange. Asymmetric oscillations in thermosolutal convection were observed by Moore *et al.* (1998) in a horizontal layer with free boundary conditions. Hollinger and Lücke (1998) have studied theoretically, in an infinite horizontal layer heated from below, the influence of the negative Soret coefficient on

stationary and traveling patterns. The current state of knowledge concerning Rayleigh-Benard convection with Soret effect was summarized by Barten *et al.* (1995). Mamou *et al.* (2001) performed a complete numerical and analytical study of double diffusive convection without Soret effect in a rectangular enclosure subject to vertical gradients of heat and solute. They showed that in a square enclosure, the flow evolves cyclically from clockwise to counterclockwise circulation and vice versa.

In the case where Ra_T and S have the same sign, i.e. when the concentration gradient opposes a destabilizing temperature gradient, steady convection is predicted. In a such case, many linear stability analyses (Legros *et al.*, 1972; Schechter *et al.*, 1974) have shown that the critical Rayleigh number goes down and asymptotically tends to zero when Ψ_S increase. Also, the critical wave number tends to zero which correspond to a large size roll at onset of convection. For cells of infinite extension or with large aspect ratio, convection is characterized by two transition points; the first is relative to the onset of convection and is characterized by small values of the Nusselt number and the second transition is characterized by an important increase in the Nusselt number accompanied by oscillation (Platten and Chavepeyer, 1976; Lhost and Platten, 1989). At this last point, the value of Rayleigh number is equal to the critical Rayleigh for the equivalent pure fluid. Recently, Mansour *et al.* (2004) performed a numerical study of the Soret effect on multiple steady-state solutions induced by double diffusive convection in a square porous cavity. It was found that, depending on the value of the Soret parameter, one, two or three solutions are possible; namely, monocellular trigonometric flow, monocellular clockwise flow and bicellular flow.

Most of the studies dealing with thermosolutal convection with Soret effect were devoted to the case of infinite or large confined horizontal layers. The objective of our study was to determine numerically the different convective behaviours in a square layer containing a saline solution heated from below with rigid and impermeable boundaries. In order to validate numerical results at the onset of convection, a linear stability study was also performed.

2. Mathematical formulation

We consider a binary mixture of incompressible fluid contained in a box of height H and length L (here we take without loss of generality the case where $H = L$). The walls of the container are assumed to be impermeable, heated from below and cooled from above with thermally insulated sidewalls (Figure 1).

The problem is described by the Navier-Stokes equations with Soret effect and with the Boussinesq-Oberbeck approximation:

$$\rho(T, C) = \rho_0(1 - \beta_T(T - T_0) + \beta_S(C - C_0)) \tag{1}$$

where $\rho_0(T_0, C_0)$ is the density of initial state:

$$\beta_T = -\frac{1}{\rho_0}\left(\frac{\partial \rho}{\partial T}\right)_C \quad \text{and} \quad \beta_S = \frac{1}{\rho_0}\left(\frac{\partial \rho}{\partial C}\right)_T$$

The x-axis is taken horizontally and the z-axis vertically upward. We introduced dimensionless variables with the help of the following scales: H for distance, H^2/κ for time, κ/H for velocity, $\kappa^2\rho_0/H^2$ for pressure, ΔT for temperature, where $\Delta T = T_1 - T_2$ and $T_0 = T_2$ is the reference temperature:
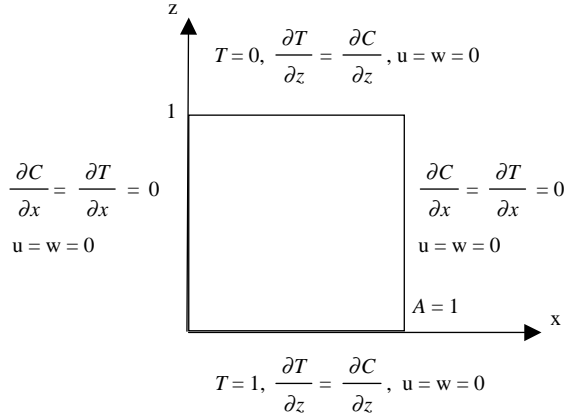
$$\Delta C = -C_0(1 - C_0)\frac{D_T}{D}\Delta T$$

Figure 1.
Scheme of the cavity configuration used in this study

for concentration and $C_0 = C_{initial}$ is the reference concentration. The separation ratio is defined by:

$$\Psi_S = \frac{\beta_S}{\beta_T} C_0 (1 - C_0) \frac{D_T}{D}$$

The dimensionless equations for conservation of momentum and of continuity could be expressed, respectively, as:

$$\nabla V = 0 \tag{2}$$

$$\frac{\partial V}{\partial t} + (V \cdot \nabla)V = -\nabla P_m + Pr\Delta V + RaPr(T + \Psi_S C)k \tag{3}$$

The dimensionless equation of energy conservation (the Dufour effect is ignored) can be expressed as:

$$\frac{\partial T}{\partial t} + (V \cdot \nabla)T = \Delta T \tag{4}$$

The dimensionless equation for the conservation of concentration with Soret effect can be written as:

$$\frac{\partial C}{\partial t} + (V \cdot \nabla)C = \frac{1}{Le}(\Delta C - \Delta T) \tag{5}$$

where:

$$Ra = \frac{g\beta_T \Delta T H^3}{\nu \kappa}, \quad Pr = \frac{\nu}{\kappa} \quad \text{and} \quad Le = \frac{\kappa}{D}$$

The boundary conditions are as follows:

$$T = 1, \quad \frac{\partial T}{\partial z} - \frac{\partial C}{\partial z} = 0 \quad z = 0 \ \forall x$$

$$T = 0, \quad \frac{\partial T}{\partial z} - \frac{\partial C}{\partial z} = 0 \quad z = 1 \ \forall x$$

$$\frac{\partial T}{\partial x} = \frac{\partial C}{\partial x} = 0 \quad x = 0, A \ \forall z$$

$$\mathbf{V} = 0 \quad z = 0, 1 \ \forall x \quad \text{and} \ x = 0, \ A \forall z \tag{6}$$

Initially, linear fields for both temperature and concentration are imposed, that is:

$$T_e = 1 - z, \quad C_e = 1 - z \quad \text{and} \ \mathbf{V}_e = 0 \tag{7}$$

The governing equations (1)-(7) were solved numerically using a finite volume method described in the following section.

2.1 Linear stability

The motionless double diffusive solution:

$$\Psi_e = 0, \quad T_e = 1 - z \quad \text{and} \ C_e = 1 - z \tag{8}$$

is particular solution of the set of equations system (1)-(7). In this paragraph, we use the stream function instead of velocity. To study the stability of this solution (8) we introduce infinitesimal perturbation defined by:

$$\psi = \Psi - \Psi_e, \quad \theta = T - T_e, \quad c = C - C_e \tag{9}$$

where (Ψ, T, C) indicate the disturbed solution and (Ψ_e, T_e, C_e) indicate the basic solution. We assume that the perturbation quantities (ψ, θ, c) are small and we ignore the smaller second-order quantities. After linearization, we obtain the following system of equations for small disturbances:

$$\frac{1}{Pr} \frac{\partial \Delta \psi}{\partial t} = \Delta^2 \psi - Ra \left[(1 + \Psi_S) \frac{\partial \theta}{\partial x} + \Psi_S \frac{\partial \xi}{\partial x} \right]$$

$$\frac{\partial \theta}{\partial t} + \frac{\partial \psi}{\partial x} = \Delta \theta \tag{10}$$

$$\frac{\partial \xi}{\partial t} + \frac{\partial \theta}{\partial t} + \frac{\partial \psi}{\partial x} = \frac{1}{Le} \Delta \xi$$

where $\xi = c - \theta$.

The dimensionless boundary conditions associated to these equations are:

$$\psi = 0, \frac{\partial \psi}{\partial z} = 0 \quad z = 0, 1 \quad \text{and} \ \psi = 0, \frac{\partial \psi}{\partial x} = 0 \quad x = 0, A$$

$$\theta = 0, \frac{\partial \xi}{\partial z} = 0 \quad z = 0, 1 \quad \text{and} \ \frac{\partial \theta}{\partial x} = \frac{\partial \xi}{\partial x} = 0 \quad x = 0, A \tag{11}$$

The solutions of system (10) with boundary conditions (11) are chosen as follows:

$$(\psi, \theta, \xi)(x, z) = (\psi(x, z), \theta(x, z), \xi(x, z)) e^{(\sigma t)} \tag{12}$$

where σ is a complex and $(\psi(x, z), \theta(x, z), \xi(x, z))$ are functions which depend on the variables x and z.

The Galerkin method was used with polynomial trial functions verifying all the boundary conditions of the problem. The polynomial trial functions are chosen as follows:

$$\psi(x,z) = \sum_{i=1}^{N}\sum_{j=1}^{M} a_{ij}\left(1-\frac{x}{A}\right)^{2}x^{i+1}(1-z)^{2}z^{j+1}$$

$$\theta(x,z) = \sum_{j=1}^{M} b_{0,j}(1-z)z^{j} + \sum_{i=1}^{N-1}\sum_{j=1}^{M} b_{ij}\,x^{i+1}\left(1-\frac{x}{A}\frac{i+1}{i+2}\right)(1-z)z^{j}$$

$$\begin{aligned}
\xi(x,z) = {} & \sum_{i=1}^{N-1} c_{i,0}\,x^{i+1}\left(1-\frac{x}{A}\frac{i+1}{i+2}\right) + \sum_{j=1}^{M-1} c_{0,j}\,z^{j+1}\left(1-z\frac{j+1}{j+2}\right) \\
& + \sum_{i=1}^{N-1}\sum_{j=1}^{M-1} c_{ij}\,x^{i+1}\left(1-\frac{x}{A}\frac{i+1}{i+2}\right)z^{j+1}\left(1-z\frac{j+1}{j+2}\right)
\end{aligned} \tag{13}$$

where N and M are positive integers numbers referred to as the truncation numbers and the a_{ij}, b_{ij} and c_{ij} are the spectral coefficients. The highest values used for N and M was $N = M = 7$. For many separation ratios values used, the truncation bigger than $N = M = 3$ is sufficient.

3. Numerical model
A finite volume method was used with the Goda projection method [20] for temporal discretization. The solution is updated by using a fully implicit method.

3.1 Temporal discretization
The Goda (1979) projection method consists of decomposing the Stokes problem into two sub-problems which are solved in two steps.

In the first step an intermediate field $\mathbf{V}^{*}$ for the velocity is predicted with an explicit field for pressure:

$$\frac{3\mathbf{V}^{*} - 4\mathbf{V}^{n} + \mathbf{V}^{n-1}}{2\Delta t} + \nabla(\mathbf{V}^{n}\mathbf{V}^{*}) - \mathbf{V}^{*}\nabla\mathbf{V}^{n} = -\nabla P_{m}^{n} + Pr\Delta\mathbf{V}^{*} + S$$

$$\mathbf{V}^{*}|_{\partial\Omega} = 0$$

where S is the source term in the equation of conservation of momentum.

In the second step, which is the projection step, we correct the velocity field predicted in step 1 to satisfy the continuity equation and we determine the pressure and velocity in time $(n+1)$:

$$\frac{3}{2\Delta t}(\mathbf{V}^{*} - \mathbf{V}^{n+1}) = \nabla\left(P_{m}^{n+1} - P_{m}^{n}\right) \quad \text{in } \Omega$$

$$\nabla\cdot\mathbf{V}^{n+1} = 0 \quad \text{in } \Omega$$

$$\mathbf{V}^{n+1}\cdot\mathbf{n} = 0 \quad \text{on } \partial\Omega$$

where Ω is inside the domain and $\partial\Omega$ is on the surface of the domain and $\mathbf{n}$ is the normal vector to $\partial\Omega$. For the equations of energy and concentration, we discredited the non-stationary term in the same way as for the equation of momentum conservation using an implicit scheme:

$$\frac{\partial T^{n+1}}{\partial t} + \nabla(\mathbf{V}^{n+1}T^{n+1}) - T^{n+1}\cdot\nabla\mathbf{V}^{n+1} = \Delta T^{n+1}$$

$$\frac{\partial C^{n+1}}{\partial t} + \nabla(\mathbf{V}^{n+1}C^{n+1}) - C^{n+1} \cdot \nabla\mathbf{V}^{n+1} = \frac{1}{Le}(\Delta C^{n+1} - \Delta T^{n+1})$$

3.2 Spatial discretization

The concentration and the temperature are calculated in the nodes of the dotted grid and the velocity components are calculated at intersection points between normal and dotted grid (Figure 2).

The equations are discredited in such a way that we obtain:

$$ANX(I,K)N_{I-1,K} + CNX(I,K)N_{I+1,K} + ANZ(I,K)N_{1,K-1} + CNZ(I,K)N_{I,K+1}$$
$$+ \left[\frac{3}{2\Delta t} - ANX(I,K) - CNX(I,K) - ANZ(I,K) - CNZ(I,K)\right]N_{I,K} = SMN(I,K)$$

where N represents variables (C, T, $\phi = P_m^{n+1} - P_m^n$, U and V) at time ($n+1$). In this case we obtain a pentagonal matrix. The inverse of the matrix is calculated using procedures form the library NSPCG (www.ma.utexas.edu/CNA/NSPCG/) based on the conjugate gradient method. In our calculations we used a boundary-fitted grid in order to be able to detect limit layers when they exist.

3.3 Code validation

In order to validate our program code, the experimental data of Lhost and Platten (1988) were used as bases of comparison. These authors used a square cell of dimensions 1:3.6:28 (and height $H = 4.15$ mm), containing a binary mixture of 90 percent water – 10 percent isopropanol heated from below. The experiments were performed at 21°C average temperature and the dimensionless parameters are as follow: $Pr = 13.2$, $Le = 140.2$ and a separation ratio $\Psi_S = -0.43$.

In the present study, we fixed $Ra = 3,300$ which corresponds to a temperature difference of $\Delta T = 275.88$ K and aspect ratio $A = 10$. In numerical analysis 250×30 grids were used, with boundary-fitted grids and a time step $\Delta t = 10^{-2}$. The temporal evolution of the vertical component of velocity in the center of the cell is recorded (Figure 3).
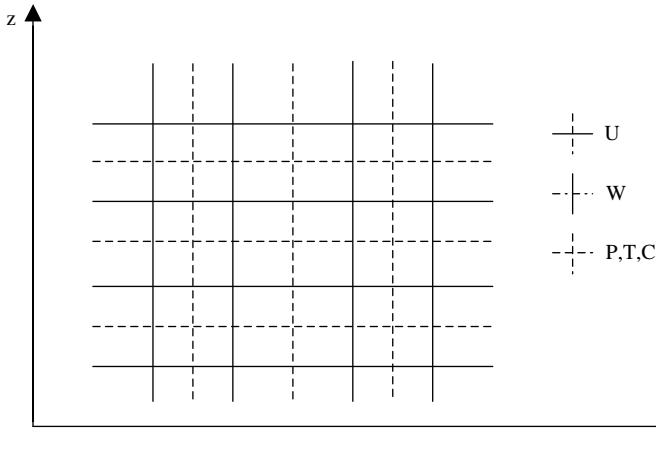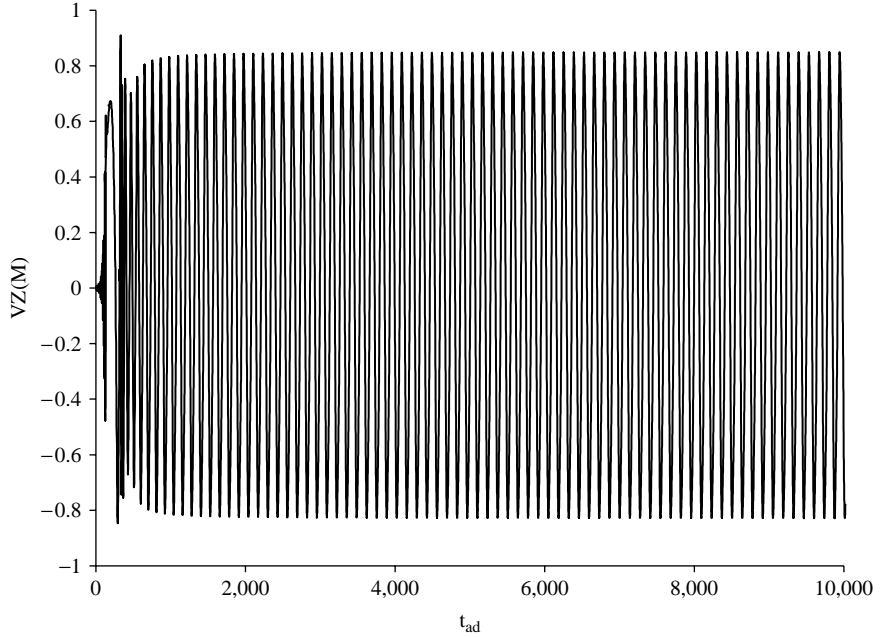

Figure 2.
The grid of spatial discretization

Figure 3.
Evolution of velocity in a point M in the middle of the cell as a function of time for $Ra = 3{,}300$, $A = 10$, $\Psi_S = -0.43$, $Pr = 13.2$ and $Le = 140.2$
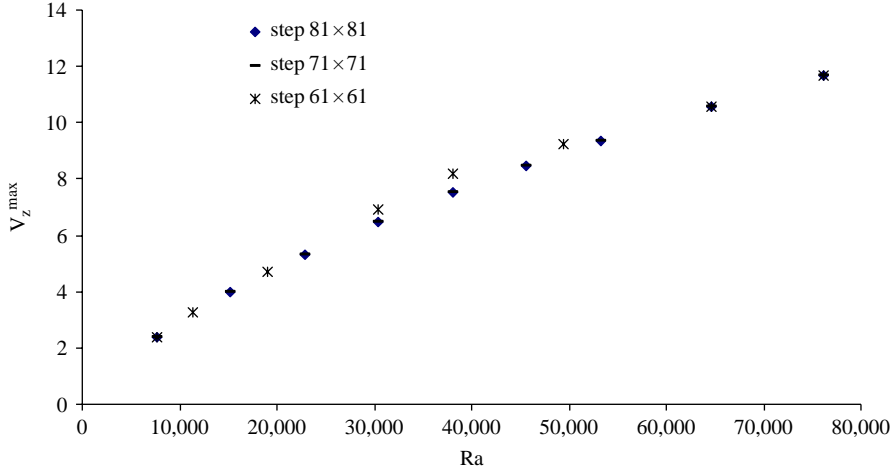
Notes: The non-dimensional Hopf frequency $F_H = 0.21$ corresponds to an non-dimensional period $\tau_{ad} = 4.65$ and the frequency of stable travelling waves $F_{TW} = 0.008$ corresponds to $\tau_{ad} = 125$. Resolution is 250×30

Lhost and Platten (1988) observed the onset of convection at the transition from $\Delta T = 275.97$ to 275.98 K, and found that the oscillation period at the convection onset is equal to 53 s (corresponding to the Hopf bifurcation periodicity). We found a dimensional period of $\tau = 49.8$ s. The period of TW was found to be $\tau_w = 1{,}337.5$ s whereas Lhost and Platten (1988) found $\tau_w = 1{,}280$ s. The difference between our value and that found by Lhost and Platten (1988) is probably due to the fact that we did not take the same aspect ratio (10 in our study against 28 in Lhost's experiment). The experiment carry out by Lhost and Platten (1988) used a cell of aspect ratio equal 28, the calculation with this aspect ratio needs an important computing time, so we have choose for our simulation an aspect ratio cell equal 10 since the effect of containment side can be neglect starting from this value.

4. Results and discussion
In the present study we considered a saline solution with 5 percent concentration in NaCl. The Prandtl and Lewis number for this solution are, respectively, $Pr = 7.6$ and $Le = 94.3$. The analysis is performed for different values of separation ratio ($\Psi_S = 0.1$, 0.0001, -0.0001 and -0.1).

In order to ensure that the results are grid size independent, we performed a grid study with three different steps (Figure 4). We found that 71×71 grid is appropriate for values of Ra less than 76,100 and a 91×91 grid for larger values of Ra. Both grids are boundary-fitted.

Figure 4.
Evolution of the vertical component of velocity as a function of Rayleigh number for three kinds of steps (61 × 61, 71 × 71 et 81 × 81)

Notes: With $\psi_S = -0.1$; $A = 1$; $Pr = 7.6$ and $Le = 94.3$

4.1 Onset of convection

In order to determine the critical Rayleigh values at the onset of convection, the calculations were started from the critical values found by the linear stability analysis. The same convective behaviors were obtained as for a cavity with a large aspect ratio or of an infinite extension. The convection onset is delayed when the separation ratio is larger (in absolute value) for negative separation ratio ($\Psi_S < 0$) and advanced for positive values of Ψ_S (Table I). An unstable state TW with Hopf frequency $\omega_H = 0.94$ is observed numerically and analytically for $\Psi_S = -0.1$ (Table I and Figure 5).

For $\Psi_S = 0.1$, we observe two bifurcation points. The first transition corresponding to the onset of convection is characterized by weak velocity while the second transition is associated to very strong increase amplitude velocity (Figure 6). When $\Psi_S = 0.0001$, the first bifurcation is not perceptible and only the second transition is identified (Figure 6).

4.2 Bifurcation diagram

The purpose is to determine the different convective behaviors in a square layer by looking at the variation of $\mathbf{V}_z^{\max}$, the maximum of the vertical component of velocity, as a function of Rayleigh number (Figure 7). The bifurcation diagram is restricted to two values of separation ratio ($\Psi_S = 0.1$ and -0.1).

Ψ_S	Linear stability study $N = M = 5$		Numerical study Resolution 71 × 71	
	Ra^{crit}	ω_H	Ra^{crit}	ω_H
−0.0001	2,623	–	2,587	–
−0.1	3,008	0.95	3,021	0.94
0.0001	2,548	–	2,549	–
0.1	166	–	160	–

Table I.
Values of critical Rayleigh number in the square cavity for different values of Ψ_S found by numerical and stability studies with $Pr = 7.6$ and $Le = 94.3$
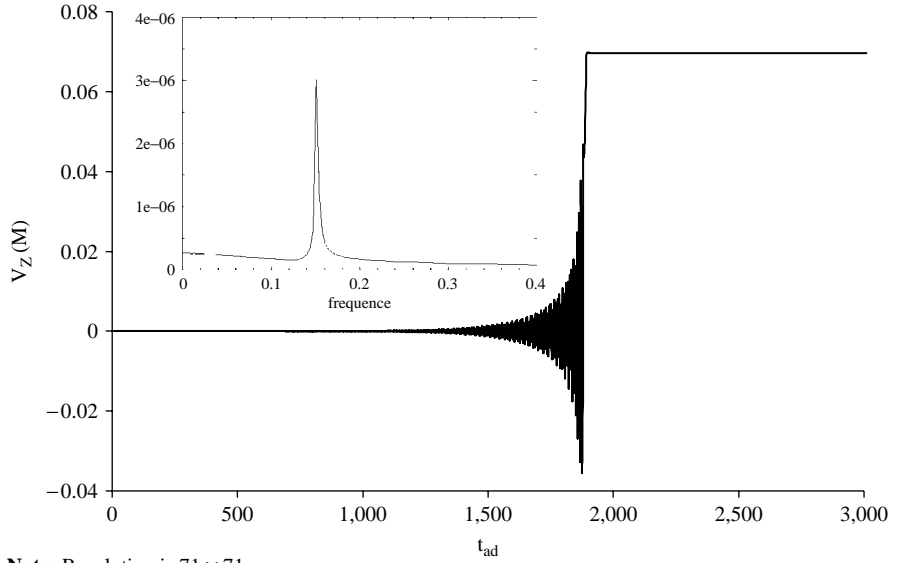
Figure 5.
Evolution of the vertical component of velocity in the middle of the cavity as a function of time au for $A = 1$, $\Psi_S = -0.1$, $Ra = 3,021$, $Pr = 7.6$ and $Le = 94.3$

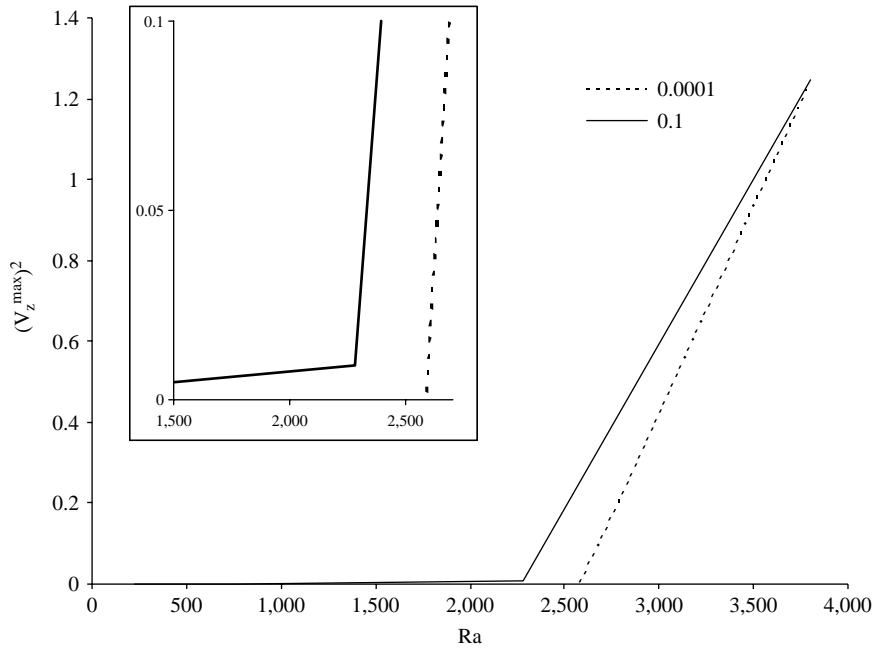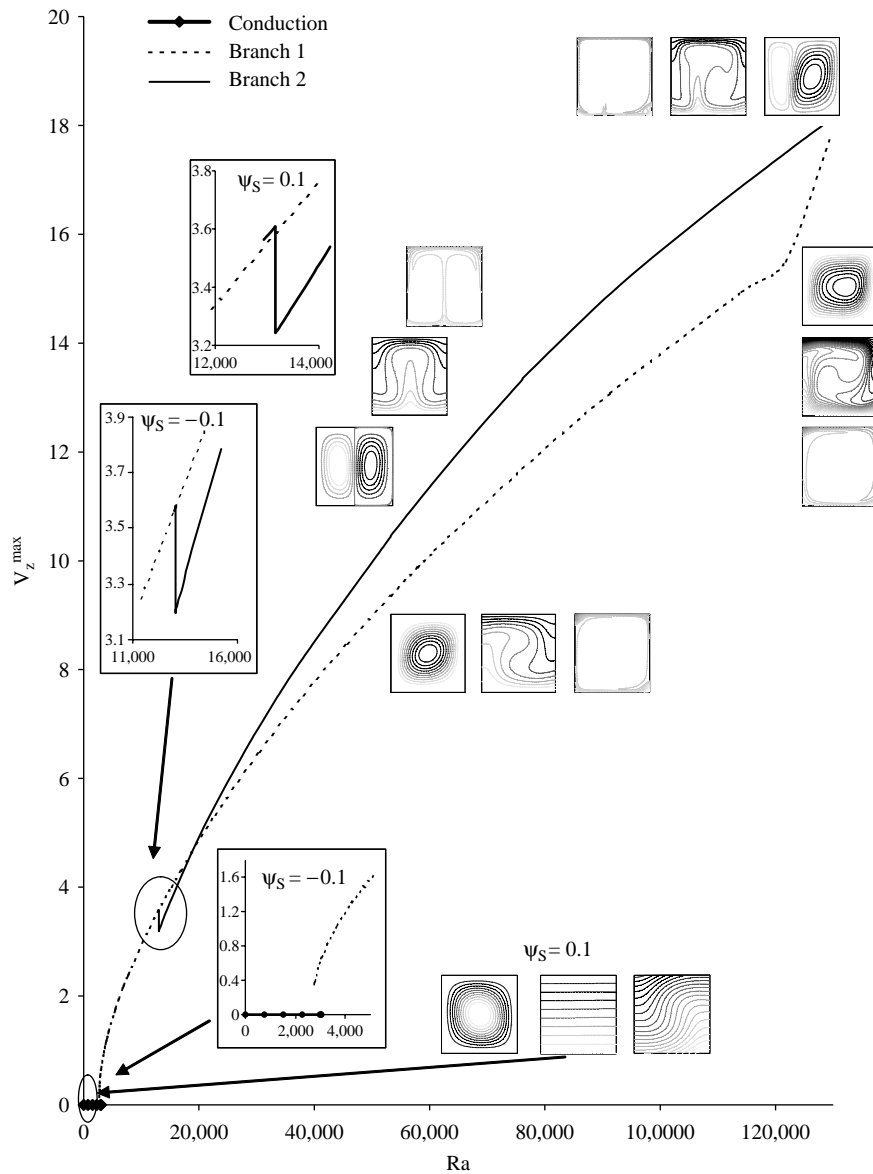**Note:** Resolution is 71×71

Figure 6.
Evolution of the vertical component of velocity as a function of Rayleigh number in the case of a square cavity $\Psi_s = 0.1$ and 10^{-4}, $Pr = 7.6$ and $Le = 94.3$

Note: Resolution is 71×71

Note: The stream function, isotherms and concentration fields for different Rayleigh numbers with $\psi_s = -0.1$ and 0.1, $Pr = 7.6$ and $Le = 94.3$

In the following, for $Ra > 7,610$, the convergent fields of velocity, concentration and temperature found for a given Ra value are used as initial fields for higher Ra values. This allows us to describe the bifurcation diagram.

From a pattern's formation perspective, at the onset of convection, the flow is characterized by a single convective roll. When the Rayleigh number is increased, the flow structure remains stable until Rayleigh number is equal to near 129,370. Furthermore, an oscillatory structure with a single roll is observed (Table II); the variation of frequency of oscillation as function Ψ_S is not that significant. For $\Psi_S = 0.1$, we found that the temperature and concentration fields at the onset of convection are similar to those of a pure fluid (Figure 7).

For high Rayleigh numbers ($Ra = 15,220$), a numerical simulation is performed using the pure diffusive fields as initial conditions. Another stationary stable flow characterized by two symmetrical contra-rotating rolls is obtained. For higher values of Ra (near $Ra = 76,100$), the symmetry of the flow is broken (Figure 8). It should be noted that when Ra decreases, the second convective branch meets the first convective branch. The value of Rayleigh number for the crossing between the two convective branches increases with Ψ_S (Table II).

For $\Psi_S = -0.1$, the results showed that a stable state of TW with low frequency ($= 0.007$) exists just below the other convective branch (Figure 9). We showed a hysteretic phenomenon at transition from the first convective branch to the conductive state.

5. Conclusions

The different convective behaviors of thermosolutal convection in a square cavity are determined numerically as a function of the separation ratio. The results confirm the existence of two stable stationary branches for any value of Ψ_S; the first convective branch is characterized by a single convective roll and ends by an oscillatory structure with a single roll. The second convective branch corresponds to two symmetrical contra-rotating rolls and for large values of Rayleigh number, asymmetric flows are observed. When $\Psi_S = -0.1$, the Hopf frequency at the onset of convection and the stable TW state, which exist at the crossing of the second to the first convective branch, are determined numerically and are in good agreement with the experimental results available.

Ψ_S	0.1	0.0001	-0.0001	-0.1
f^{osc}	0.24	0.25	0.24	0.26
$Ra^{2 \to 1}$	13,158	13,051	13,079	13,028

Notes: The values of oscillation frequency for $Ra = 129,370$ (f^{osc}) and Rayleigh number for the crossing between the two convective branches ($Ra^{2 \to 1}$) for different values of Ψ_S. With $A = 1$, $Pr = 7.6$ and $Le = 94.3$

Table II.

$Ra = 91{,}320$ $Ra = 2{,}43{,}520$
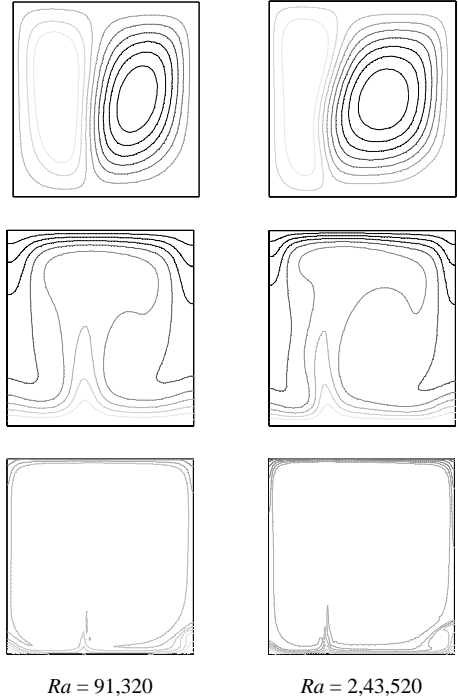
Note: With $A = 1$; $Pr = 7.6$ and $Le = 94.3$

Figure 8.
Stream function,
isotherms and
iso-concentration for two
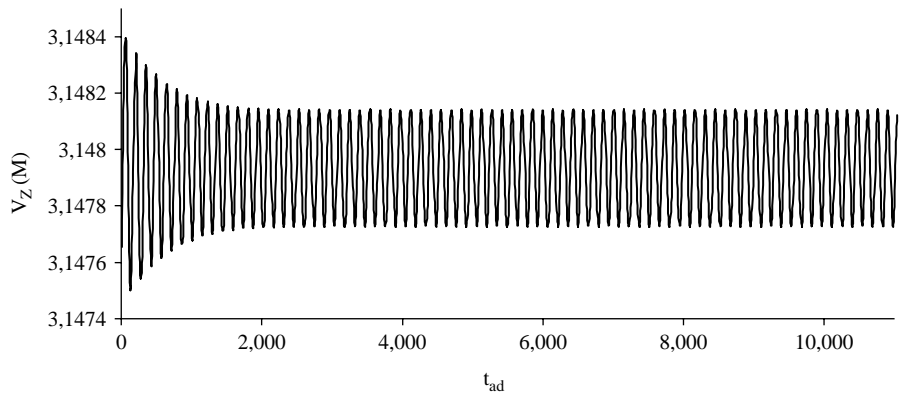values of Ra and
$\Psi_S = -0.1$

Figure 9.
Evolution of the vertical
component of velocity in
the middle of the cavity as
a function of time for
$A = 1$, $\Psi_S = -0.1$,
$Ra = 13{,}032$, $Pr = 7.61$
and $Le = 94.3$

References

Barten, W., Lücke, M., Kamps, M. and Schnitz, R. (1995), "Convection in binary fluid mixture I. Extended traveling-wave and stationary states", *Phys. Rev. E*, Vol. 51, pp. 5636-61.

Goda, K. (1979), "A multistep technique with implicit difference schemes for calculating two- or three-dimensional cavity flows", *Journal of Computational Physics*, Vol. 30, pp. 76-95.

Heinrichs, R., ahlers, G. and Cannell, D.S. (1987), "Travelling waves and spatial variation in the convection of a binary mixture", *Phy. Rev. A*, Vol. 35, p. 2761.

Hollinger, St. and Lücke, M. (1998), "Influence of the Soret effect on convection of binary fluids", *Phy. Rev. E*, Vol. 57, p. 4238.

Hurle, D.T. and Jakeman, E. (1971), "Soret driven thermosolutal convection", *J. Fluid Mech.*, Vol. 47, pp. 667-87.

Knobloch, E. (1986), "Oscillatory convection in binary mixtures", *Phys. Rev. A*, Vol. 34, p. 1538.

Legros, J.C., Platten, J.K. and Poty, P. (1972), "Stability of a two-component fluid layer heated from below", *Phys. Fluids*, Vol. 15, p. 1383.

Lhost, O. and Platten, J.K. (1988), "Transition between steady state traveling waves and modulated waves in the system water-isopropanol heated from below", *Phy. Rev. A*, Vol. 38, pp. 3147-50.

Lhost, O. and Platten, J.K. (1989a), "Experimental study of the transition from nonlinear traveling waves to steady overturning convection in binary mixture", *Phy. Rev. A*, Vol. 40, pp. 4552-7.

Lhost, O. and Platten, J.K. (1989b), "Large-scale convection induced by the Soret effect", *Phys. Rev. A*, Vol. 40, pp. 6415-20.

Mamou, M., Vasseur, P. and Hasnaoui, M. (2001), "On numerical stability analysis of double-diffusive convection in confined enclosures", *J. Fluid Mech.*, Vol. 437, pp. 209-50.

Mansour, A., Amahmid, A., Hasnaoui, M. and Bourich, M. (2004), "Soret effect on double-diffusion multiple solution in a square porous cavity subject to cross gradients of temperature an concentration", *Int. Comm. Heat Mass Transfer*, Vol. 31, pp. 431-40.

Moore, D.R., Weiss, N.O. and Wilkins, J.M. (1998), "Asymmetric oscillation in thermosolutal convection", *J. Fluid Mech.*, Vol. 233, p. 561.

Nield, D.A. (1967), "The thermohaline Rayleigh-Jeffres problem", *J. Fluid Mech.*, Vol. 29, pp. 545-58.

Platten, J.K. and Chavepeyer, G. (1976), "Instabilité et flux de chaleur dans le problème de Bénard à deux constituants aux coefficients de Soret positives", *Int. J. Heat and Mass Transfer*, Vol. 19, pp. 27-32.

Rehberg, I. and Ahlers, G. (1985), "Experiment observation of a codimension-two bifurcation in a binary fluid mixture", *Phys. Rev. Lett.*, Vol. 55, pp. 500-3.

Schechter, R.S., Prigogine, I. and Hamm, J.R. (1972), "Thermal diffusion and convective instability", *Phys. Fluid*, Vol. 15, pp. 379-86.

Schechter, R.S., Velarde, M.G. and Platten, J.K. (1974), "The two-component Bénard problem", *Adv. Chem. Phys.*, Vol. 26, pp. 265-301.

Veronis, G. (1965), "On infinite amplitude instability in thermohaline convection", *J. Mar. Res.*, Vol. 23, p. 1.

Veronis, G. (1968), "Effect of stabilizing gradient of solute on thermal convection", *J. Fluid Mech.*, Vol. 34, pp. 315-36.

Corresponding author
A. Mojtabi can be contacted at: mojtabi@cict.fr